



In situ spectroelectrochemistry and cytotoxic activities of natural ubiquinone analogues

Wei Ma^a, Hao Zhou^a, Yi-Lun Ying^a, Da-Wei Li^a, Guo-Rong Chen^a, Yi-Tao Long^{a,*}, Hong-Yuan Chen^{b,*}

^aShanghai Key Laboratory of Functional Materials Chemistry and Department of Chemistry, East China University of Science and Technology, 130 Meilong Road, Shanghai 200237, PR China

^bDepartment of Chemistry, Nanjing University, 22 Hankou Road, Nanjing 210093, PR China

ARTICLE INFO

Article history:

Received 23 April 2011

Received in revised form 2 June 2011

Accepted 10 June 2011

Available online 16 June 2011

Keywords:

Ubiquinone/coenzyme Q

Electrochemistry

ESR

In situ spectroelectrochemistry

Cytotoxicity

ABSTRACT

Quinones are a group of potent antineoplastic agents. Here we described effective and facile routes to synthesize a series of ubiquinone analogues (**UQAs**). These unique compounds have been investigated by electrochemistry and *in situ* UV–vis spectroelectrochemistry to explore their electron-transfer processes and radical properties in aprotic media. The structure–activities relationships of inhibiting cancer cell proliferation of **UQAs** were examined in murine melanoma B16F10 cells using a 72 h continuous exposure MTT (3-(4,5-dimethylthiazol-2-yl)-2,5-diphenyltetrazolium bromide) assay. Our results revealed that **UQAs** had improved antiproliferative activity and displayed better inhibitory effects than natural ubiquinone 10. The cytotoxic activities of **UQAs** were correlated to the semiubiquinone radicals, which were confirmed by *in situ* electron spin resonance (ESR). In the cytotoxicity test, 6-vinylubiquinone **5** and 6-(4'-fluorophenyl) ubiquinone **7** that possess half maximal inhibitory concentration value (IC₅₀) of 6.1 μM and 6.2 μM. This would make them as valuable candidates for future pharmacological studies.

© 2011 Published by Elsevier Ltd.

1. Introduction

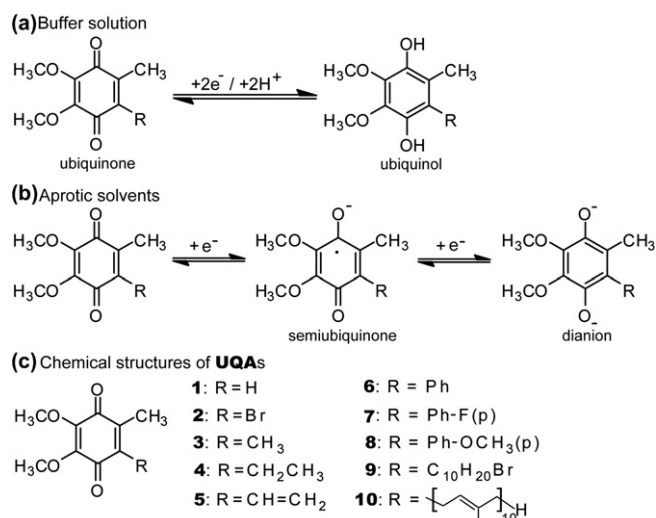
The ubiquinones, also known as coenzyme Q_n, constitute essential cellular components of all phylogenetic branches of life. The various kinds of ubiquinones are distinguished by their number of isoprenoid units, which are composed of the redox active ubiquinonyl ring with a tail of isoprenoid units ($n=1-12$) in different homologue forms occurring in nature.^{1–3} Ubiquinone 10 is the predominant form found in humans and most mammals, which is located predominantly at the hydrophobic core of the phospholipid bilayer of the inner membrane of the mitochondria. As an essential cofactor in the electron transport chain, it shuttles the electrons between complex I (or complex II) and complex III.^{4,5} In the photosynthetic reaction centers, ubiquinone serves as a mobile electron and proton carrier transferring electrons and protons from the reaction centers to other components of the bioenergetic cycle.^{6,7}

In addition to the enzymological importance, the pharmaceutical activities and the nutritional importance of ubiquinone 10 have been revealed to indicate that ubiquinone serves versatile functions in living systems.^{2,8} Most of such biological functions are associated with the redox activity of ubiquinone. The ubiquinones and their intermediates semiubiquinones, as well as reduced forms

ubiquinol exist inside hydrophobic cell membranes. It is advantageous to study their electrochemical properties in trace water environment, such as aprotic organic solvents, which mimic the nonpolar environment in a living cell where the electrochemical properties differ from that observed in aqueous systems.⁹ In buffer solution, the redox chemistry of ubiquinone shows a well-documented two electron, two proton transfer process, giving the ubiquinol as the final product.^{9,10} However, in dry aprotic media, the ubiquinone is reduced to form the semiubiquinone radical anion ($Q^{\cdot-}$) and in a second step accepts another electron to produce the ubiquinone dianion (Q^{2-}).^{9,10} The electrochemical reduction mechanism of ubiquinone in different solvents is shown in Scheme 1a and b. In aprotic solvents, the monoanion and dianions could undergo strong hydrogen-bonding with trace water.¹¹ The details for electrochemical reduction mechanism of ubiquinone in unbuffered solution and aprotic solvents with trace water can be seen in Supplementary data.

Although the synthesis and their biological applications of coenzyme Q₁₀ in recent years are diverse and well established, there are very few examples of systemic ubiquinone analogues (**UQAs**) studies for electron transfer and biological application.^{12–16} For example, Yu and co-workers demonstrated that when ubiquinone acts as an electron acceptor for succinate-ubiquinone reductase, an alkyl side chain of six or more carbons gives maximum activity; whereas an alkyl side chain of 10 or more carbons gives maximum activity when ubiquinone is an electron donor for ubiquinol/

* Corresponding authors. Tel./fax: +86 21 642 50032; e-mail addresses: ytlong@ecust.edu.cn (Y.-T. Long), hychen@netra.nju.edu.cn (H.-Y. Chen).



Scheme 1. Chemical structures of synthesized **UQAs** and their electrochemical reduction mechanism in different solvents.

cytochrome c reductase.¹² On the other hand, the electron-transfer activity of ubiquinone, to serve as an electron/proton carrier, differs significantly by the effects of side chain variations and the arrangement of the substituents on the ubiquinonyl ring.¹⁶ It is important to note that a modification in the direct substitution pattern on the ubiquinonyl ring impacts its capability to accept electrons and, thus, its capacity to mediate biological reactions.

A number of studies have examined the protective effects of **UQAs** as antioxidants,^{2,8} which hints at the prospect of employing **UQAs** as drugs. But little work has been done on the systematic design of **UQAs** as anticancer drugs targeted toward inhibiting the tumor cell growth. Here we present a preliminary study that the relationship between structure and anticancer activities of **UQAs**. We developed facile methods to synthesize a series of **UQAs** that contain the following substituents in the 6-position: hydrogen, halide, alkyl, vinyl, and aryl, as shown in **Scheme 1c**. The alkyl substituted compounds 6-methylubiquinone **3** and 6-ethylubiquinone **4** were synthesized starting from commercially available ubiquinone 0. The alkyl residue was introduced by a radical Hundsdiecker decarboxylation of acetic acid/propanoic acid using silver nitrate and peroxydisulfate in the degassed acetonitrile/water mixture.¹⁷ The alkyl substituted ubiquinones were obtained in only one step, although the yield was low (20%). The synthesis of 6-vinylubiquinone **5** was carried out by a Wittig coupling-reaction.¹⁸ In addition, the three aromatic substituted ubiquinones **6**, **7**, **8** were obtained by palladium-mediated Suzuki coupling-reactions.^{19,20} The target products were obtained by two steps using 6-bromoubiquinone **2**²¹ and the corresponding boronic acids with high yields. The 6-(10-bromodecyl) ubiquinone **9** was synthesized using 11-bromoundecanoic acid and ubiquinone 0.²²

The electrochemical study of **UQAs** was performed in aprotic organic media as well as the full characterization of the electrochemically generated semiquinone radical anionic species by *in situ* UV-vis and electron spin resonance (ESR) spectroelectrochemistry. Furthermore, we also studied the bioactivity of **UQAs** against tumor cells to develop key structure-property-activity relationships on the basis of their intrinsic chemical interests. 10 **UQAs** (**1–10**) were studied against murine melanoma B16F10 cells by the standard microplate colorimetric MTT assay. These compounds were designed to obtain structure-bioactivity relationships arising from the effect of substituent group at 6-position on cytotoxicity. These cytotoxic data provide a valuable insight to select potential candidates for further development of **UQAs** as anticancer drugs *in vitro*.

2. Results and discussion

2.1. Electrochemical characteristics

The electrochemical measurements of the **UQAs** were carried out by using cyclic voltammetry (CV) and differential pulse voltammetry (DPV) techniques. **Fig. 1** illustrates the cyclic voltammetric responses at glassy carbon (GC) electrode in 75 mM tetrabutylammonium perchlorate (TBAP) CH₃CN solution containing 0.5 mM of **UQAs** at various scan rates. The scanning range of potential is between -2.2 and 0.2 V versus Ag/AgCl. The initial scan started from ~ 0.2 V versus Ag/AgCl. The values of formal potential for all **UQAs** during the redox process, for the first step producing the semiquinone radical ($Q^{\cdot-}/E_{c1}$) and then further reducing to the dianion (Q^{2-}/E_{c2}) at more negative potentials (corrected for iR drop in the cell) at GC electrode versus Ag/AgCl are given in **Table 1**.

As shown in **Fig. 1**, the redox peak potentials for different **UQAs** are substantially different under the same conditions. As expected, several trends are clear from the CVs in **Fig. 1**. First, all **UQAs** reveal two couples of redox peaks, which correspond to two successive single electron-transfer processes to give mono- and dianionic species^{8,9} in aprotic CH₃CN solutions, as shown in **Scheme 1b**. Cathodic to anodic peak-to-peak separations were typically 65–70 mV for the first process and about 80–100 mV for the second process at a scan rate of 100 mV s⁻¹. With increasing the scan rate, peak-to-peak separations for the two redox processes diverged slightly, which gives a clear indication of reversible for first redox process and quasi-reversible for the second process in this system.²³ The second trend in the CVs is the ratio of cathodic peak current to the anodic peak current for the first redox process is close to unity for all **UQAs**, throughout the scan rate range from 20 to 200 mV s⁻¹, which further confirms that it is a reversible process. However, the ratio of peak currents for the second redox process was found to be 0.85–0.95 at scan rate of 100 mV s⁻¹, indicating quasi-reversibility. Third, it can be seen that the height of the second peak is less than that of the first peak in the CVs of all **UQAs**, suggesting chemical reactions may occur in the second reduction steps of **UQAs**. Among several mechanisms considered in attempted simulations, the assumption involving adsorbed species been discarded, reduction of a dimer formed by the reaction between two semiquinones, and the complexation reaction between ubiquinones and their dianions has been proposed.^{9,24} Similar phenomenon also exists in other quinones.^{9,23,24} However, it is important to note that even though the suggested complexation or chemical reaction affected the peak currents significantly, it turned out to have no effect on the reduction potentials.²⁴ The increase of scan rate promoted an increase of current peak in both oxidation and reduction reactions. The anodic peak and cathodic peak shift to more positive potential and more negative potential, respectively, as the scan rate increased from 20 to 200 mV s⁻¹ in **Fig. 1**. The detailed description of the relationship between peak currents and scan rates is shown in a plot (see inset in **Fig. 1**). Both anodic and cathodic peak currents vary approximately linearly with the square root of the scan rate over the range of 20–200 mV s⁻¹, which suggests that the process is predominantly diffusion controlled.²⁵ However, all zero intercept and the negligible change in shape of voltammograms at higher scan rates are indications for no complex mass transport conditions involving trapped solution and linear diffusion.

Further redox information was obtained by carrying out DPV under the same conditions, which is a more sensitive electrochemical technique. As shown in **Fig. 2**, **UQAs** exhibit the expected two reduction peaks, also attributing to two-step single-electron redox process. The different ubiquinones show variation of the peak potential values in the same experimental condition, which could be explained by the electronic effects of the substituents. It is

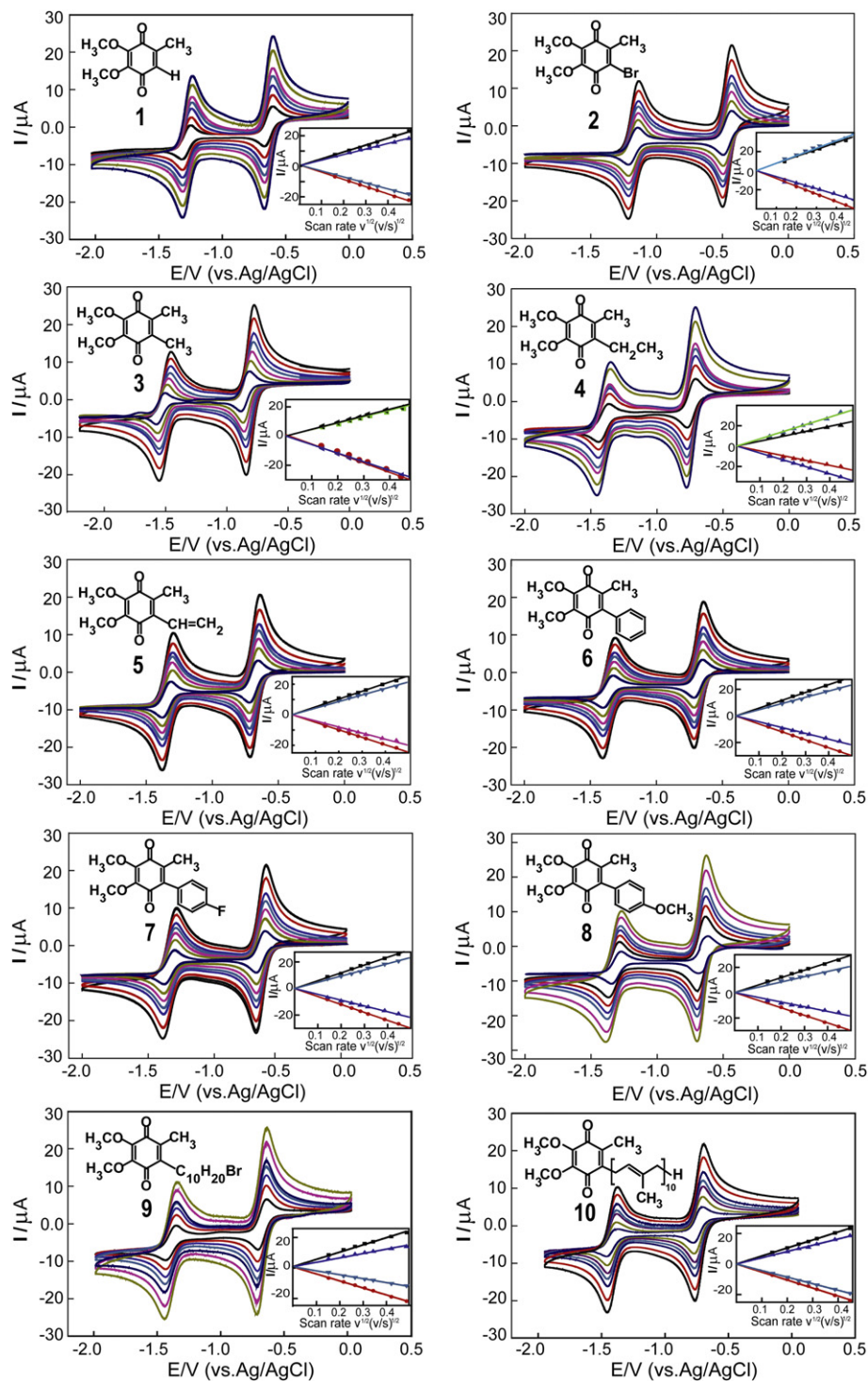


Fig. 1. Cyclic voltammograms of 0.5 mM **UQAs** obtained at GC electrode (~ 3 mm in diameter) in distilled CH_3CN containing 75 mM TBAP at different scan rates of 20, 40, 60, 80, 100, 150, and 200 mV s^{-1} . The inset shows the linear increasing of the redox peak current depends on increasing the square root of the scan rate.

expected that the substitutional change on the ubiquinonyl ring, either by an electron-withdrawing group or an electron-donating group, has a dramatic impact on the redox properties of **UQAs**, as the corresponding redox potentials shifted positively or negatively by hundreds of millivolts. The substitutional differences on **UQAs** have obvious effect on electron density at the ubiquinonyl ring and thus influence their electron affinity. Compound **2**, having the electron-withdrawing group (bromo) on the ubiquinonyl ring, and **3** with electron-donating group (methyl) were investigated in

Fig. 2. The reduction of **3** was more difficult than that of **1** as evidenced by the fact that the reduction potential of **3** appeared at -0.771 and -1.480 V, respectively, which are more negative than those for **1**, i.e., -0.650 and -1.327 V, respectively. The reduction potential of **2** was -0.524 and -1.266 V, which illustrates that the reduction of **2** was more favorable than that of **1**. The potential variation of **3** and **4** is hardly distinguishable for second peak, but **3** had a slightly more positive reduction potential than **4** for the first electron-transfer step. It shows that electron-donating effects of

Table 1
Cathodic and anodic peak potentials (V), UV–vis absorbance (nm) and cytotoxicity (μM) of ubiquinone analogues

Ubiquinone analogues	Formal potential/V				UV–vis absorbance/nm			Cytotoxicity (IC_{50} , μM)
	E_{a1}^a	E_{a2}^a	E_{c1}^b	E_{c2}^b	Q^c	Q^{-d}	Q^{2-e}	
Ubiquinone 0 (1)	−0.580	−1.230	−0.650	−1.327	263, 400	320, 412, 439	320	24.8±3.1
6-Bromoubiquinone (2)	−0.476	−1.172	−0.524	−1.266	288, 425	319, 416, 442	324	15.9±2.3
6-Methylubiquinone (3)	−0.708	−1.384	−0.771	−1.480	273, 409	320, 417, 442	320	20.4±2.4
6-Ethyl ubiquinone (4)	−0.723	−1.388	−0.786	−1.412	275, 425	321, 417, 443	321	21.9±2.7
6-Vinylubiquinone (5)	−0.640	−1.288	−0.713	−1.372	302, 415	303, 357, 454	366	6.1±1.1
6-Phenylubiquinone (6)	−0.648	−1.316	−0.717	−1.406	265, 312, 401	320, 420, 444	325	12.8±1.1
6-(4'-Fluorophenyl) ubiquinone (7)	−0.628	−1.280	−0.697	−1.376	263, 314, 406	318, 423, 443	327	6.2±1.0
6-(4'-Methoxyphenyl) ubiquinone (8)	−0.660	−1.328	−0.726	−1.426	267, 351, 450	320, 421	328	10.3±1.1
6-(10-Bromodecyl)-ubiquinone (9)	−0.639	−1.351	−0.716	−1.448	275, 417	321, 417, 422	322	48.3±3.3
Ubiquinone 10 (10)	−0.699	−1.380	−0.765	−1.452	273, 419	321, 413, 440	317	>100

^a Anodic peak potential versus Ag/AgCl at scan rate of 100 mV s^{−1}.

^b Cathodic peak potential versus Ag/AgCl at scan rate of 100 mV s^{−1}.

^c UV–vis absorbance peak value for ubiquinone material.

^d UV–vis absorbance peak value of semiquinone.

^e UV–vis absorbance peak value of ubiquinonyl dianion.

methyl and ethyl on ubiquinonyl ring was almost identical. Based on the previous work, we knew that conjugated system can promote the transfer ability of electron.²⁶ To validate this possibility, we investigated the voltammetric behaviors of **5**, the ubiquinone with the rigid alkyl side chains. The formal reduction potentials of **5** were −0.713 and −1.372 V, respectively, while corresponding potentials for **4** were −0.786 and −1.412 V. Consequently, it demonstrates that the electron-transfer activity of ubiquinone with a rigid alkyl side chain would be more favorable than ubiquinone with flexible alkyl side chains. The reduction potentials of 6-aryl ubiquinones were investigated in order to characterize the change in redox behavior associated with substitutional change on the aromatic ring (not directly on ubiquinonyl ring). Furthermore, the expected electrochemical behaviors were observed with **6**, **7**, and **8** in Fig. 2.

Generally, the inductive effect is great when the substituent is located closely and vice versa. The slight difference of reduction potentials (−0.717 and −1.406 V for **6**, −0.697 and −1.376 V for **7**, −0.726 and −1.426 V for **8**) arising from changes of substituent effects on aromatic ring, are qualitatively smaller than the effects of groups attached directly to ubiquinonyl ring. The variations of the potential could be correlated to the electron withdrawing or donating character of substitutional change on the ubiquinonyl ring. Therefore, the ubiquinones with electron-withdrawing groups exhibit substantially positive potential shifts, while ubiquinones with electron-donating group possess more negative potential values.²⁷ As clearly shown in Fig. 2, the height of second reduction peak with different degree is less than that of the first peak for the ten UQAs. This also suggests a chemical reaction, which could be correlated with electronic effects of the substituent, may occur in the second electrochemical step of UQAs.

In this study, the oxidation potentials for reduced product of UQAs also followed the harmony with the electronic nature of the substituent and remained the same as observed for the two-step single-electron electrochemical process.^{28,29}

2.2. In situ UV–vis spectroelectrochemistry

The information of the semiquinone anions of UQAs in aprotic solvent has not been fully characterized by electrochemical performance. In order to further investigate the deeper changes in radical intermediates (semiquinone) and final reduced species (dianion) as indicated by their electrochemical properties, we explored the corresponding effects of UQAs on their electronic transitions by *in situ* UV–vis spectroelectrochemical experiments. The UV–vis spectra were recorded during the reduction of UQAs in CH_3CN containing TBAP in an optically transparent thin layer

electrochemical cell. As the reduction of UQAs with constant potential, a substantial change in the UV–vis spectra was observed. Fig. 3 shows the characteristic spectra of UQAs before and after electrochemical reduction.

Before reduction, UQAs exhibit the characteristic bands as shown in black line of Fig. 3. The UV–vis spectra of three aromatic substituted ubiquinones **6**, **7**, and **8** displayed long wavelength absorption bands with comparable intensity at 312, 314, and 350 nm, respectively. The absorption bands can be assigned to $\pi-\pi^*$ transitions of the aryl-substituent.³⁰ The stronger absorptions at shorter wavelengths and the relative weak absorptions at the longer wavelength are an indication of the $\pi-\pi^*$ and $n-\pi^*$ electronic transitions of the ubiquinonyl rings³⁰ at 265 nm and 415 nm, 263 nm and 410 nm, 267 nm and 430 nm, respectively. As can be seen from the Fig. 3, **5** displayed a strong absorption band at 302 nm. It was the overlapped result of the $\pi-\pi^*$ transition of the conjugated vinyl group and the $\pi-\pi^*$ transition of the ubiquinonyl ring. Absorption spectral studies show that the effect of overlapped peak led to a red shift together with a wider absorption band than others. The relative weak absorption at 415 nm is assigned to the $n-\pi^*$ electronic transition of the ubiquinonyl ring.³⁰ However, the UQAs with non-aromatic substitutions **1**, **2**, **3**, **4**, **9**, and **10** do not display the absorption bands at 310–350 nm, which are assigned to the $\pi-\pi^*$ transitions of the aromatic ring in black line of Fig. 3. The UV–vis spectra of these UQAs illustrate strong diagnostic absorption bands at 260–300 nm, which correspond to the $\pi-\pi^*$ transition in the ubiquinonyl systems. The spectra also contain relative weak and broad absorption bands at 400–425 nm which are an indication of the $n-\pi^*$ electronic transitions of the ubiquinonyl rings.

With the application of a first reduction potential of E_{c1} in Table 1, one-electron participated in the reduction of UQAs. As shown in red line of Fig. 3, after the first reduction step, the characteristic absorption bands at 260–290 nm disappear and were replaced by a sharp and intense absorbance at around 320 nm, which are attributed to the $\pi-\pi^*$ absorption spectra of ubiquinonyl ring converting to aromatic ring.²⁷ In particular, the strong absorption band at 302 nm of **5** is still kept except appearance of new peak at 355 nm, which correspond to the $\pi-\pi^*$ transition of the conjugated vinyl group and the $\pi-\pi^*$ absorption spectra of ubiquinonyl ring converting to aromatic ring. In red line of Fig. 3, the new wide absorption bands appear at 410–450 nm are assigned to the $n-\pi^*$ absorption spectra of semiquinone radicals. This indicates that ubiquinones were converted to the semiquinone radicals.²⁷

With the application of a more negative potential at E_{c2} in Table 1, semiquinone anions were reduced and accepted another electron (two electron overall). The band of the semiquinone radicals disappears and the corresponding dianionic characteristic

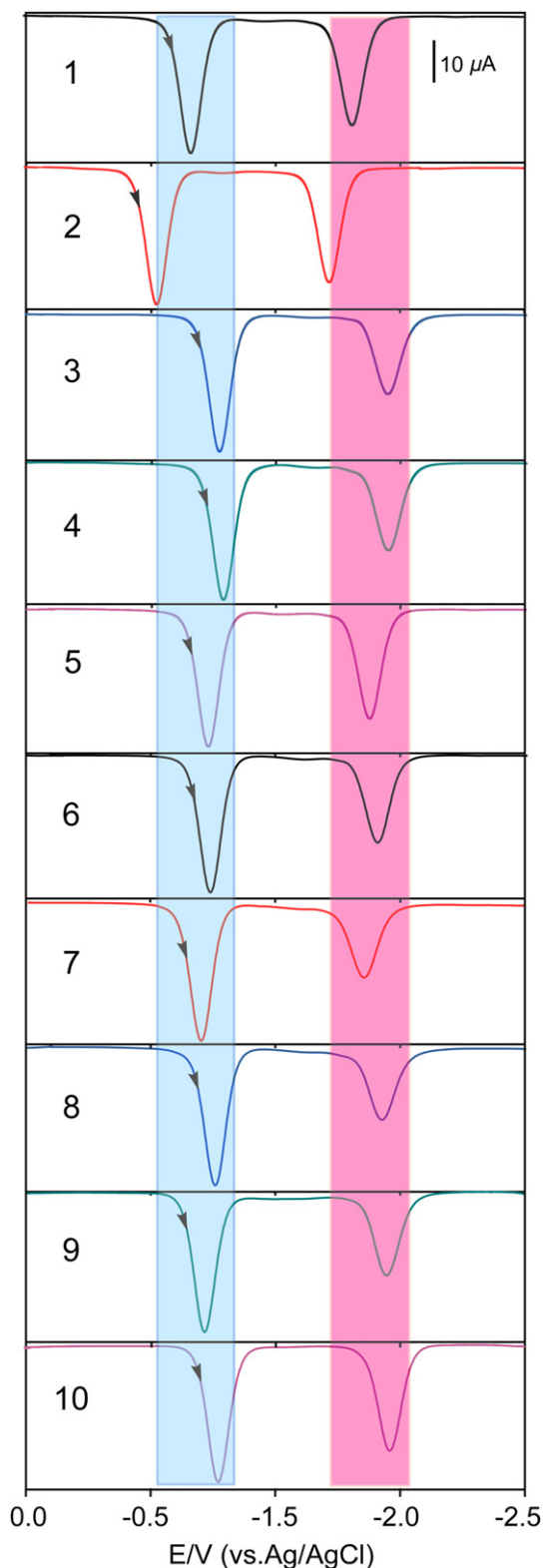


Fig. 2. Differential pulse voltammetry (DPV) curves of 0.5 mM **UQAs** obtained at GC electrode in CH_3CN containing 75 mM TBAP during reduction process, the potential is from 0.2 to -2.5 V with a pulse amplitude of 50 mV and a sample pulse width of 100 ms. Arrow indicates initial scan direction.

absorbance bands of **UQAs** located at about 320 nm were found,²⁷ as shown in green line of Fig. 3. The absorbance of 6-vinylubiquinone **5** was observed at 366 nm. Although similar in shape of absorption bands of other **UQAs**, it differed significantly regarding its wavelength, which is attributed to an interference of vinyl bond.

On the basis of the electrochemical and spectroscopic results in Figs. 1 and 3, a mechanism can be proposed for the generations of the reduced species in aprotic CH_3CN solution. The electron-transfer steps could occur consecutively with the constant potential reduction. After applying a first reduction potential of E_{c1} , the initial one-electron reduction of **Q** (oxidation state of **UQAs**) produced $\text{Q}^{\cdot-}$ (semiubiquinones), which could be further reduced by accepting another electron to form Q^{2-} (dianion) immediately applied a second reduction potential of E_{c2} . The spectroscopic experiments indicate that the state of **UQAs** is influenced by the different reduction potentials, and thus the UV–vis spectra display different extremes. It is confirmed that the substitutional change on the ubiquinonyl ring, such as aromatic ring or vinyl bond, has a dramatic impact on characteristic bands, as the corresponding absorption peak value or shape. The assignment of all absorption bands from UV–vis spectra of **UQAs** with their reduced intermediate and final species at various potentials are summarized in Table 1.

2.3. Cytotoxicity test

The redox properties of ubiquinone play critical roles in their therapeutic and toxicological properties. In its reduced form (ubiquinol), ubiquinone may function as a class of potentially interesting drug of antioxidant and free radical scavengers.^{2,16} However, recent demonstrations show that ubiquinones may provide another possibility of indirect antioxidant function.³¹ Many quinones possess cytotoxic properties that made them useful anticancer and antibacterial drugs. Adriamycin is a good case in point as an effective antitumor therapeutical agent.³² Consequently, there is a high prospect of development of ubiquinone based cytotoxic agents. With this anticipation our designed **UQAs** were subjected to cytotoxicity testing to determine if a structure–activity relationship could be identified.

In vitro experiments to determine cytotoxicity were performed on a series of synthesized **UQAs** using a 72 h continuous exposure MTT assay³³ against B16F10 murine melanoma cell line. Results were expressed as a percentage of viability of cells grown in the absence of drug, but also with 3% DMSO medium. Cytotoxicity (IC_{50}) was defined as the concentrations of **UQAs** (**1–10**) corresponding to 50% tumor cell viability of the untreated control in the absence of an inhibitor and was calculated from three independent experiments. All IC_{50} values are μM values, for B16F10 cell were shown in Table 1. In this study, the compound was thought to be ineffective against the growth of murine melanoma cells when IC_{50} value >100 μM . As shown in cytotoxicity assays (Fig. 4), the cytotoxic effect of the **UQAs** is directly related to their structural characteristics of substituent including chain length, functional groups, aryl ring, and degree of saturation. The result of cytotoxicity test showed that **UQAs** decreased the viability and proliferation of tumor cells in a dose-dependent manner, but at different sensitivities. All **UQAs** were active at micromole concentration levels to induce the death of tumor B16F10 cells, but the cytotoxicity was completely lost when ubiquinone **10** was used. Fig. 4 clearly demonstrates that synthesized **UQAs** can effectively inhibit tumor growth under experimental conditions with an IC_{50} value.

In the cytotoxicity test, **5** and **7** are most active, and possess IC_{50} value of 6.1 and 6.2 μM , respectively. Comparison of the compounds with and without the substituents which belong to π electron conjugated system with ubiquinonyl ring (entries **5–8**, Table 1) indicate that the presence of the conjugated system led to a marked increase in cytotoxicity. For instance, a vinyl group presented at the 6-position of ubiquinonyl ring, activity increased in the inhibition of B16F10 tumor cell growth, compared with ethyl groups in the corresponding position (IC_{50} values of **4** and **5** was 21.9 and 6.1 μM , respectively). The same trend can be observed for compounds **6**

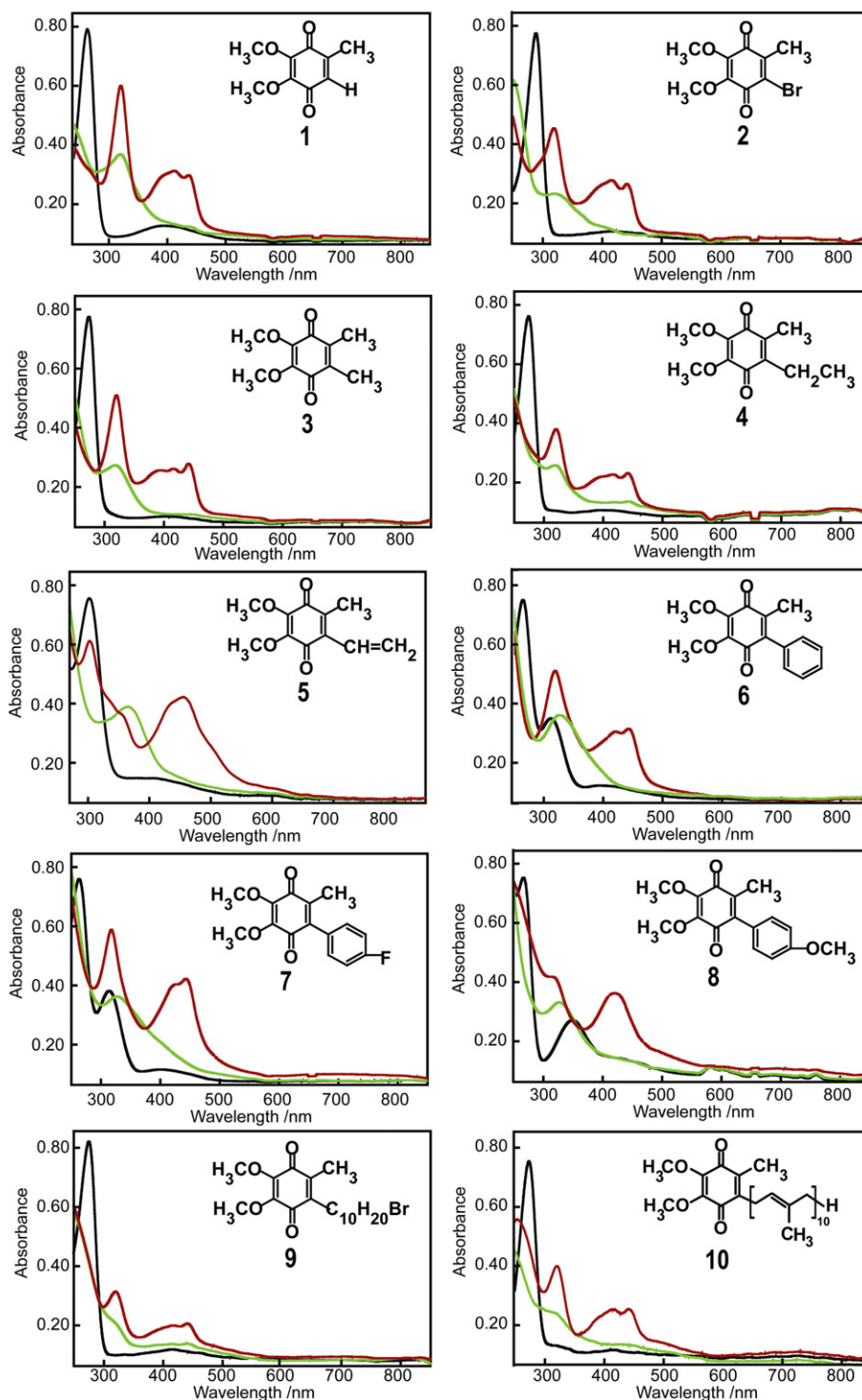


Fig. 3. *In situ* UV–vis spectroelectrochemistry obtained in an optically transparent thin layer electrochemical cell during the constant potential reduction of 0.2 mM **UQAs** in aprotic CH_3CN contained 30 mM TBAP (black line: the UV–vis spectra of oxidation state of ubiquinone; red line: the UV–vis spectra of semiquinone were obtained after applying a first reduction potential of E_{R1} ; green line: the UV–vis spectra of ubiquinonyl dianion were obtained after applying a second reduction potential of E_{R2}).

($\text{IC}_{50}=12.8 \mu\text{M}$), **7** ($\text{IC}_{50}=6.2 \mu\text{M}$) and **8** ($\text{IC}_{50}=10.3 \mu\text{M}$), which show higher activity on cytotoxicity. This result discloses that compounds containing aromatic rings were more active than compounds containing aliphatic chains against the growth of murine melanoma cells. In other words, the compounds with conjugated system were more active than compounds with non-conjugated system. Moreover, as the compounds **6**, **7**, and **8** have a slight difference in the structure, which of them contain a subset similar to aromatic

ring, cytotoxicity against murine melanoma B16F10 cells appeared less difference. This was also particularly evident in many properties of electrochemistry and *in situ* UV–vis spectroelectrochemistry shown in the Figs. 1 and 2. Compounds **1** ($\text{IC}_{50}=24.8 \mu\text{M}$), **2** ($\text{IC}_{50}=15.9 \mu\text{M}$), **3** ($\text{IC}_{50}=20.4 \mu\text{M}$), **4** ($\text{IC}_{50}=21.9 \mu\text{M}$), and **9** ($\text{IC}_{50}=48.3 \mu\text{M}$) exhibit mild to moderate activity. The observation indicates that the compounds with longer chain show less activity to inhibit the growth of murine melanoma B16F10 cells than the

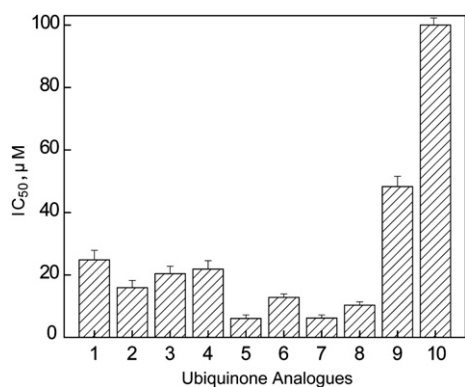


Fig. 4. IC₅₀ values of UQAs (1–10) toward B16F10 murine melanoma cell were determined by MTT assay over an exposure of 72 h.

corresponding those of shorter side chain. In the Fig. 4, we clearly observed that **2** showed higher anticancer activity than **9**. A similar relationship can be observed if compounds **3** and **4** were considered, although there was only a negligible variation in structures.

It will be important to have data concerning the toxicity of these molecules against normal cells to have an idea about the safety window as anticancer agent. We demonstrated a high toxicity of UQAs against murine melanoma cells, while at the same concentrations they were low toxicity for normal cell (human umbilical vein endothelial cells). The details as described in Supplementary data. In this study, the results of cytotoxicity test revealed that synthesized UQAs (1–9) were capable of inducing a decrease of tumor B16F10 cell growth and have greater effects against tumor cell growth than natural product **10**. The major differences were observed for UQAs with different substituents indicates that the presence of the conjugated system with ubiquinonyl ring (for example, aryl ring or vinyl bond) led to a striking enhancement in cytotoxicity. Further studies using other model compounds are required to better understand structure–activity relationships, but these are the first step to investigate such properties of ubiquinone. The experimental result of cytotoxicity test highlights that a series of ubiquinone compounds are worthy of the further investigation, it would provide us the information to get better understanding of relationship between the side chain effects of UQAs and the biological activities.

2.4. *In situ* ESR spectroelectrochemistry

Anticancer experimental therapeutics show that quinone undergo enzymatic reduction via one or two electrons to give the corresponding semiquinone radical or hydroquinone anion as part of their mechanism of cell death induction.^{34–36} To investigate the possible link between radical and cytotoxicity of ubiquinone compounds, we chose four typical ubiquinone compounds, **5**, which was the most active, **2**, **6**, which exhibited mild activity and **10**, which was inactive against the growth of murine melanoma cell line.

In situ ESR spectroelectrochemical experiments were carried out for these ubiquinone compounds. The radical intermediate anions of UQAs (semiquinones) characterized by ESR were prepared *in situ* by electrochemical reduction in CH₃CN. At the applied potential corresponding to the first reduction peak obtained from the cyclic voltammetric experiments, the corresponding ESR signals were observed and recorded with the time. The investigated UQAs formed stable paramagnetic intermediates after the first reduction step with well-resolved ESR signals in CH₃CN. The ESR spectra of the radical anion of UQAs show the variation of the ESR signal intensity with the electrolysis time in Fig. 5. As a versatile technique

for detecting paramagnetic species, ESR is very sensitive to the structure of the substituent even in much closed conformation. The nuclei in the substituents of UQAs split the ESR lines and affected the behavior of their radicals, resulting in the characteristic ESR spectra. The substitutional effects on the electronic structures of the semiquinone radical anion species are obvious. Different ESR signals for four UQAs may also be attributed to the substitutional change leading to localization of the charge and then spin onto the ubiquinone moiety. With applying the potential close to the first reduction of UQAs, the intensity of semiquinone radical anion species for **2**, **5**, **6**, and **10** has been progressively increased, as shown in Fig. 5.

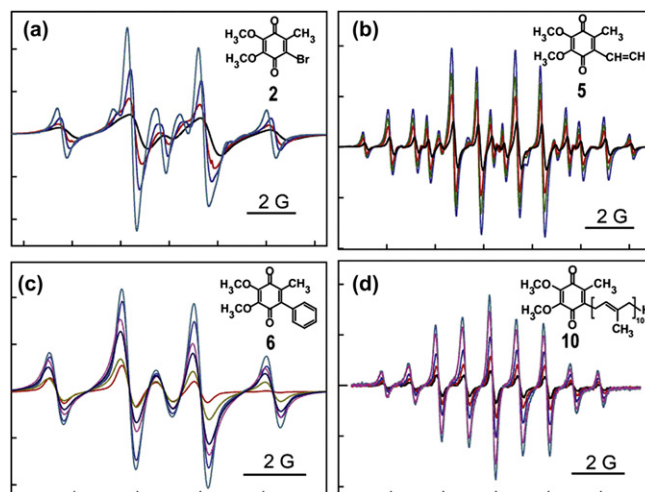


Fig. 5. Increase in the intensity of ESR spectra of four UQAs (**2**, **5**, **6**, and **10**) with electrolysis time.

To obtain further information about semiquinone radicals and cytotoxicity, relative radical intensity of ESR signals with decay time was used. When the intensity of semiquinone radical maintained nearly a constant value with increase of electrolysis time, the applied potential was removed. In the Fig. 6, it was observed that the ESR signal gradually decreased with decay time. This indicates that semiquinone radicals were converted to ubiquinones and their disproportionated species.³⁷ The rate of variation of ESR signal intensity as a function of decay time for four UQAs was significantly different. In the Fig. 6, the rate of radical decay of **10** was much faster than others, which showed that more radical anions quenched per unit time. It is interesting to note that the more cytotoxic active compound **5** and **6** has the longer decay

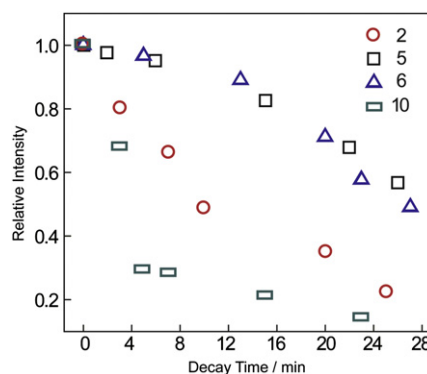


Fig. 6. The relative intensity variation of semiquinone radicals of UQAs (**2**, **5**, **6**, and **10**) with decay time.

time for semiquinone radical decay, indicating that the radical anion of **5** and **6** was more stable. The trend of radical decay of **UQAs 2** and **10** are also in good agreement with cytotoxic study. The cytotoxic activities of present compounds against the growth of murine melanoma cell line versus their intensity variation of semiquinone radical anions showed a linear relationship with decay time. Such a correlation suggests the cytotoxic activities depend upon the stability of semiquinone radical. This area deserves further research, but our reported results only hint the relationship between cytotoxic activity and semiquinone radical anion.

3. Conclusions

In conclusion, the effective and facile synthetic routes for **UQAs** have allowed the full investigation of electrochemical, UV–vis, ESR spectroelectrochemical properties and the biological activities of these compounds. The degree of electron transfer in aprotic media was estimated from CV and DPV. This study shows that **UQAs** undergo two sequential single-electron reductions to give the mono- and dianion at the surface of GC electrode in distilled aprotic media. As seen from Figs. 1 and 2, different substituents on the ubiquinonyl ring of 6-position produce significant effect on the electron-transfer activity of **UQAs**. It is also demonstrated that the UV–vis spectra of a series of **UQAs** accurately predict electron-transfer reactions as well as the effect of structural changes on spectra.

Quinones are a kind of important additions to the repertoire of compound as a strategy for the treatment of cancer and have potentials as anticancer agents. Given the documented elevation in many tumor types, especially those cancers with few treatment options, such as melanoma carcinoma, the continued exploration of the therapeutic utility is critical. Transcripts profiling from IC₅₀ value of growth suppress on murine melanoma B16F10 cells indicates that synthesized **UQAs** induce tumor cell death. In the cytotoxicity test, 6-vinylubiquinone **5** and 6-(4'-fluorophenyl) ubiquinone **7** are the most active, possessing IC₅₀ value of 6.1 and 6.2 μM, respectively and IC₅₀ value of ubiquinone **10** is >100 μM. To our astonishing, synthesized **UQAs** have a more potent ability to inhibit tumor cell growth than natural product ubiquinone **10**. Results of these studies may help to develop insights in this emerging area of interest in order to further explore the relationship between the side chain of **UQAs** and the biological activities. In an effort to define their mechanism of action, we evaluated cytotoxic activities by *in situ* ESR. The ability of ubiquinone compounds induced to death of cancer cell is relative with the decay time of semiquinone radical. It is noteworthy that more cytotoxic active compounds **5** and **6** have longer decay time of semiquinone radical.

Notably, it is believed that our route of the structure–bioactivity relationship can be used to select potential candidates for further development of **UQAs** as anticancer drugs.

4. Experimental section

4.1. Chemicals

HPLC grade acetonitrile (CH₃CN) and other analytical grade reagents were purchased from Sigma–Aldrich. Tetrabutylammonium perchlorate (98%) (TBAP) were purchased from Aldrich; Coenzyme Q₀ were of the best available grade (>98%) from Sigma; N₂ (99.998%, prepurified) was obtained from Cryogenic Gases (Detroit, MI). All chemical reagents for synthesis were of analytical grade, obtained from commercial suppliers, and used without further purification unless otherwise noted. All electrodes for electrochemical experiments were purchased from Shanghai Chenhua Co., Ltd., China.

4.2. Electrochemistry

HPLC grade CH₃CN was initially dried by distilling over CaH₂ before use. All solutions for electrochemistry were dried by placing the solvent, electrolyte, and **UQAs** inside a 25 mL vacuum syringe (Yikang Medical Instrument Group Co. Ltd, Jiangxi, China) containing 3 Å molecular sieves (that were dried under vacuum at 240 °C for 12 h) and storing the syringe under a dry nitrogen atmosphere for at least 48 h. During the measurement, a dry nitrogen purge maintains an oxygen and moisture free environment. A standard jacketed three-electrode cell was used for electrochemistry. A Pt electrode and a Ag/AgCl electrode were used as counter electrode and reference electrode, respectively. The measurement of approximate 0.5 mM **UQAs** was carried out at glassy carbon (GC) electrode (~3 mm diameter) in CH₃CN test solution. Immediately before use, the working electrode was polished with alumina suspension and rinsed with ultrapure water, then rinsed with acetone and dried with N₂. The electrolyte solution was 75 mM TBAP in CH₃CN test solution. Accurate potentials were obtained using ferrocenium/ferrocene as an internal standard. The temperature was controlled by using 25 °C circulating water bath through the outer cell jacket. Cyclic voltammograms were recorded at from 20 to 200 mV s⁻¹. The measurements were performed at CHI 660 electrochemical workstation (Shanghai Chenhua Co., Ltd., China).

4.3. *In situ* UV–vis spectroelectrochemistry

The UV–vis spectrum was recorded during reduction of **UQAs** in an optically transparent thin layer electrochemical cell (optical path length is 0.4±0.1 mm) via an Ocean Optics DT-minutesi-2 halogen recourse and USB2000+ spectrometer. The cell featured a platinum net working electrode and salt bridge to a platinum wire counter electrode and Ag/AgCl reference electrode. Electrochemistry during the UV–vis spectral measurement was controlled by CHI 1232A electrochemical workstation (Shanghai Chenhua Co., Ltd., China). **UQAs** solutions were prepared by dissolving **UQAs** in aprotic CH₃CN solution containing TBAP. The prepared solutions were deoxygenated for 30 min prior to each experiment and the cell was kept under a nitrogen atmosphere throughout the experiment.

4.4. Cytotoxicity test using MTT assay

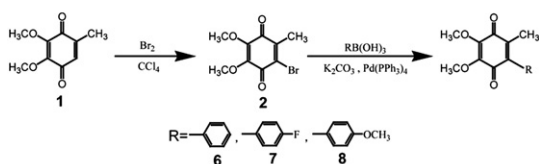
Cytotoxicity of **UQAs** on murine melanoma B16F10 cells and human umbilical vein endothelial cells was determined using the standard microplate colorimetric MTT assay. MTT is a yellow tetrazolium salt: 3-(4,5-dimethylthiazol-2-yl)-2,5-diphenyltetrazolium bromide. The MTT test is a colorimetric assay, that is, used to quantify spectrophotometrically the amount of living cells, due to the reduction of MTT to purple formazan by the mitochondria of the living cell. Experiments of the cell viabilities of different samples were performed on the cell cultures for 14–16 days. The murine melanoma B16 cells in log phase were trypsinized (0.01%) and seeded in 96-well plates at a density of 2.0×10³ cells/well. The cells were incubated at 37 °C under 5% CO₂ for 24 h. Murine melanoma B16 cells were cultured for 72 h under regular growth conditions with samples of six different concentrations, respectively. Briefly, the cultures were incubated with medium for 3 h at 37 °C after addition of 20 mL MTT (5 mg/mL). The supernatant was removed and dimethyl sulfoxide (DMSO) was added to each well to dissolve the formazan crystals. Afterward, the solution from each well was transferred to a 96-well plate. The absorbance values were read on a Molecular Devices Spectra MAX 340 at 550 nm with background subtraction at 690 nm. The IC₅₀ value was calculated at 50% of the cell growth using at least two separate replicates.

4.5. *In situ* electron spin resonance (ESR) spectroelectrochemistry

ESR measurements were performed in the X-band region with a Bruker EMX-8/2.7 spectrometer at room temperature. The potential during the ESR measurements was controlled with CHI 1232A electrochemical workstation. Silver wire was used as the working electrode and the length of it matched the height of the ESR cavity. An alloy wire electrode and a Ag/AgCl electrode served as the counter electrode and the reference electrode, respectively. ESR scan parameters used the following: microwave frequency 9.87 GHz, modulated frequency 100 kHz, modulated amplitude 0.15 G, time constant 81.92 s, conversion time 163.84 s. UQAs solutions were used for *in situ* ESR spectroelectrochemical experiments. These solutions were prepared by dissolving the desired ubiquinone compounds in aprotic CH₃CN containing TBAP. The prepared solutions were deoxygenated for 30 min prior to each experiment and the cell was kept under a nitrogen atmosphere throughout the experiment.

4.6. Synthesis of ubiquinone analogues (UQAs)

THF was distilled freshly from benzophenone/sodium ketyl under a nitrogen atmosphere. CH₃CN was degassed in the ultrasonic cleaner with degas function. ¹H and ¹³C NMR spectra were recorded on a Bruker FT-500 MHz spectrometer at room temperature. Mass spectra (EI) were recorded on an MA1212 instrument using standard conditions. All reactions were monitored by thin layer chromatography (TLC) using silica-coated plates and visualizing under UV light. Light petroleum of the distillation range 60–90 °C was used. Evaporation of solvents was performed at reduced pressure, using a rotary evaporator. Column chromatographic experiments were performed with Silica Gel (300–400 mesh) (Scheme 2).



Scheme 2. Synthesis of 6-bromoubiquinone **2** and 6-arylubiquinone **6**, **7**, **8**.

4.6.1. 6-Bromoubiquinone (2). To a stirred solution of coenzyme Q₀ **1** (10.60 g, 58.0 mmol) in 120 mL of carbon tetrachloride was added dropwisely bromine (10.52 g, 68.0 mmol) at room temperature²¹ (see Scheme 2). The reaction mixture was stirred for 4 h, and then treated with water, dried with magnesium sulfate, and evaporated. The reaction mixture was purified by column chromatography to give **2** (81%) as red needle crystals. ¹H NMR (500.0 MHz, CDCl₃, 298 K): 3.95 (s, 3H, –OCH₃), 4.05 (s, 3H, –OCH₃), 2.22 (s, 3H, –CH₃) ppm.

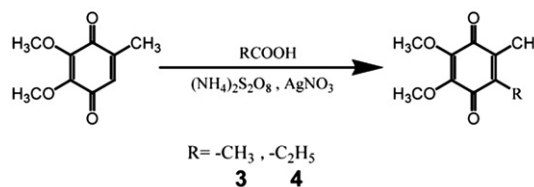
4.6.2. 6-Arylubiquinone (6–8). To a mixture of **2** (1.0 mmol), boric acid (0.13 g, 1.0 mmol), Pd(PPh₃)₄ (3.0 mol%) were added CHCl₃ (8.5 mL) and aqueous K₂CO₃ (1.5 mL, 2 mmol) under argon atmosphere^{19,20} (see Scheme 2). The reaction mixture was refluxed overnight under 60 °C. After cooling to room temperature, ice cooled water (10 mL) was added and then the reaction mixture was extracted with CH₂Cl₂ (3×10 mL). The organic layer was washed with brine, dried (Na₂SO₄), filtered, and concentrated in vacuum. The residue was purified by column chromatography to afford the corresponding compound (**6–8**) as dark purple oily substances.

4.6.3. 6-Phenylubiquinone (6). ¹H NMR (500.0 MHz, CDCl₃, 298 K): 3.95 (s, 3H, –OCH₃), 4.05 (s, 3H, –OCH₃), 1.95 (s, 3H, –CH₃),

7.05–7.15(m, 2H, ArH), 7.40–7.50 (m, 3H, ArH) ppm; MS (EI): 258.1, found: 258.09.

4.6.4. 6-(4'-Fluorophenyl)ubiquinone (7). ¹H NMR (500.0 MHz, CDCl₃, 298 K): 3.95 (s, 3H, –OCH₃), 4.05 (s, 3H, –OCH₃), 1.95 (s, 3H, –CH₃), 7.08–7.15 (m, 4H, ArH) ppm; ¹³C NMR (125.7 MHz, CDCl₃, 298 K): 184.5 (C=O), 184.1 (C=O), 164.3 (C, Ar–F), 145.3 (C, Ar), 145.1 (C, Ar), 144.8 (C, Ar), 144.5 (C, Ar), 140.3 (C, Ar), 140.1 (C, Ar), 132.3 (C, Ar), 127.5 (C, Ar), 115.3 (C, Ar), 61.2 (2× –OCH₃), 12.9(–CH₃) ppm; HRMS (ESI): calcd for C₁₅H₁₄O₄F [M+H]⁺ 277.0870, found 277.0870.

4.6.5. 6-(4'-Methoxyphenyl)ubiquinone (8). ¹H NMR (500.0 MHz, CDCl₃, 298 K): 3.95 (s, 3H, –OCH₃), 4.05 (s, 3H, –OCH₃), 1.95 (s, 3H, –CH₃), 6.95(m, 2H, ArH), 7.05(m, 2H, ArH), 3.85 (s, 3H, –ArOCH₃) ppm (Scheme 3).



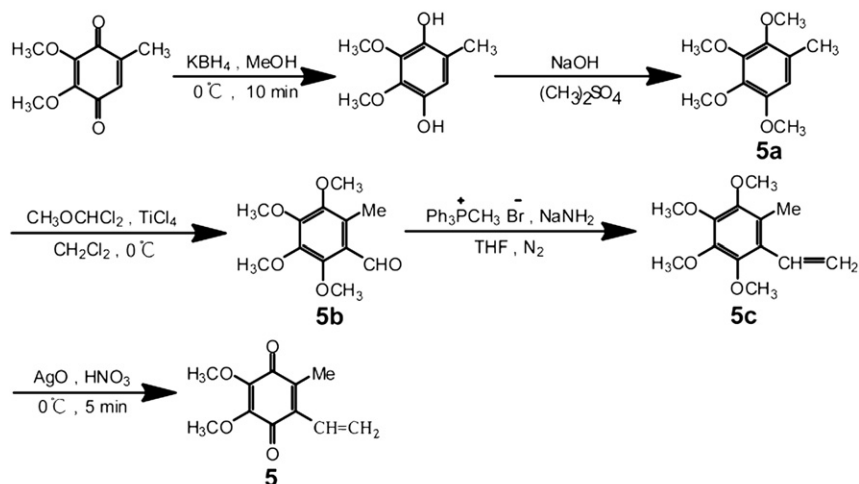
Scheme 3. Synthesis of 6-methylubiquinone **3** and 6-ethylubiquinone **4**.

4.6.6. 6-Ethylubiquinone (4). To a solution of coenzyme Q₀ **1** (1.00 g, 5.4 mmol) in degassed CH₃CN (120 mL) at 25 °C were added AgNO₃ (0.25 g, 1.5 mmol) and propanoic acid (0.48 g, 6.5 mmol). After the mixture was heated to 65 °C, (NH₄)₂S₂O₈ (2.80 g, 12.5 mmol) in 10 mL degassed H₂O was added dropwisely over 30 min¹⁷ (see Scheme 3). After 3 h, the reaction mixture was cooled to 25 °C and was extracted with EtOAc (3×150 mL), and the organic layers were washed with brine (150 mL), dried (MgSO₄), and concentrated. The crude product was purified by silica chromatography to give **4** (20%). ¹H NMR (500.0 MHz, CDCl₃, 298 K): 3.99 (s, 3H, –OCH₃), 4.00 (s, 3H, –OCH₃), 2.02 (s, 3H, –CH₃), 1.05 (t, 3H, –CH₂CH₃), 2.45 (q, 2H, –CH₂CH₃) ppm.

4.6.7. 6-Methylubiquinone (3). The same method for synthesizing **4**. ¹H NMR (500.0 MHz, CDCl₃, 298 K): 3.99 (s, 6H, 2× –OCH₃), 2.02 (s, 6H, 2× –CH₃) ppm; MS (EI): 196.1, found: 196.07 (Scheme 4).

4.6.8. 2,3,4,5-Tetramethoxytoluene (5a). To a solution of coenzyme Q₀ **1** (4.00 g, 21.7 mmol) in methanol (30 mL) at 0 °C was dropwise added a solution of KBH₄ (5.85 g, 108.5 mmol) in methanol (30 mL). After 10 min, the reaction was quenched by the addition of EtOAc and then 5% aqueous HCl^{38,39} (see Scheme 4). The mixture was extracted with EtOAc (3×50 mL) and the organic layer was washed successively with water and brine, dried (MgSO₄), and evaporated at reduced pressure. The crude hydroquinone (4.20 g) was dissolved in EtOH (20 mL) and to this solution at room temperature was added a solution of NaOH (2.20 g in 6 mL H₂O) and dimethyl sulfate (5.30 mL, 56.0 mmol) with cooling in a ice water bath in six portions simultaneously. After 45 min, 5% aqueous HCl was added and the mixture was extracted with EtOAc (3×50 mL). The organic layer was washed successively with water and brine, dried (MgSO₄), and evaporated to give **5a** (74%) as a light yellow liquid.⁴⁰ ¹H NMR (500.0 MHz, CDCl₃, 298 K): 3.99 (s, 12H, 4× –OCH₃), 2.25 (s, 3H, –CH₃), 6.45(s, 1H, ArH) ppm.

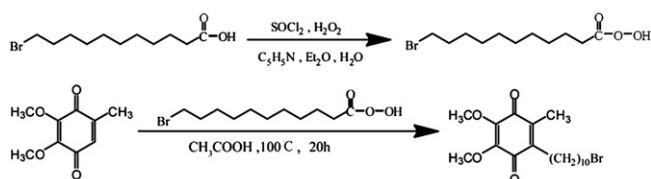
4.6.9. 2,3,4,5-Tetramethoxy-6-methylbenzaldehyde (5b). To a stirred solution of **5a** (4.24 g, 20 mmol) in CH₂Cl₂ (30 mL) was added dichloromethyl methyl ether (6.89 g, 60 mmol) at 0 °C followed by addition of TiCl₄ (11.38 g, 60 mmol)⁴¹ (see Scheme 4). The resulting

Scheme 4. Synthesis of 6-vinylubiquinone **5**.

mixture was stirred for 4 h at ambient temperature and then poured into ice water. After stirring vigorously for 10 min, the organic layer was separated. It was washed with water, dried, and evaporated. The residue was chromatographed on silica gel to give **5b** (90%) as a light yellow liquid. $^1\text{H NMR}$ (500.0 MHz, CDCl_3 , 298 K): 3.99 (s, 12H, 4 \times $-\text{OCH}_3$), 2.25 (s, 3H, $-\text{CH}_3$), 10.45 (s, H, $-\text{CHO}$) ppm.

4.6.10. 2,3,4,5-Tetramethoxy-6-methylstyrene (5c). To a mixture of triphenylmethylphosphonium bromide (5.71 g, 16 mmol) and sodium amide (0.78 g, 20 mmol) was added dry THF (50 mL) and stirred for 12 h at room temperature in the atmosphere of argon. The yellow supernatant liquid was added through a syringe to the solution of **5b** (3.07 g, 12.8 mmol) in dry THF (10 mL) under the protection of argon¹⁸ (see Scheme 4). The reaction mixture was stirred for 24 h at room temperature and then quenched with 2% aqueous HCl and extracted with EtOAc (3 \times 30 mL). The organic extracts were washed with water, dried, and evaporated. The residue was chromatographed on silica gel to give **5c** (75%) as a white solid. $^1\text{H NMR}$ (500.0 MHz, CDCl_3 , 298 K): 3.95 (s, 6H, 2 \times $-\text{OCH}_3$), 3.80 (s, 6H, 2 \times $-\text{OCH}_3$), 2.25 (s, 3H, $-\text{CH}_3$), 5.50 (m, 2H, $=\text{CH}_2$), 6.70 (m, 1H, $-\text{CH}=\text{C}$) ppm.

4.6.11. 6-Vinylubiquinone (5). To a solution of the compound **5c** (0.02 g, 0.8 mmol) in THF (14 mL), silver(II) oxide (0.49 mg) and 6 N HNO_3 (1 mL) were added. After being stirred for 5 min at 0 °C, silver(II) oxide (2.00 g) and 6 N HNO_3 (2 mL) were further added⁴² (see Scheme 4). The reaction mixture was stirred at room temperature for 30 min and was purified by column chromatography to give **5** (77%) as red needle crystals. $^1\text{H NMR}$ (500.0 MHz, CDCl_3 , 298 K): 3.99 (s, 6H, 2 \times $-\text{OCH}_3$), 2.25 (s, 3H, $-\text{CH}_3$), 5.80 (m, 2H, $=\text{CH}_2$), 6.60 (m, 1H, $-\text{CH}=\text{C}$) ppm; $^{13}\text{C NMR}$ (125.7 MHz, CDCl_3 , 298 K): 184.7 (C=O), 184.2 (C=O), 144.3 (C, Ar), 143.1 (C, Ar), 141.1 (C, Ar), 148.7 (C, Ar), 133.6 ($-\text{CH}=\text{C}$), 121.6 ($=\text{CH}_2$), 61.2 (2 \times $-\text{OCH}_3$), 12.9 (2 \times $-\text{CH}_3$) ppm (Scheme 5).

Scheme 5. Synthesis of 6-(10-bromodecyl)ubiquinone **9**.

4.6.12. 6-(10-Bromodecyl)ubiquinone (9). 11-Bromoundecanoic acid (4.00 g, 15.1 mmol) and SOCl_2 (1.6 mL, 21.5 mmol) were heated at 90 °C for 15 min. Excess SOCl_2 was removed by distillation under reduced pressure and the residue was dissolved in diethyl ether (20 mL) and cooled to 0 °C. Hydrogen peroxide (30%, 1.8 mL) was added, followed by dropwise addition of pyridine (1.4 mL) over 45 min, then diethyl ether (10 mL) was added.²² After 1 h at room temperature, the product was diluted with diethyl ether (150 mL), washed with H_2O (2 \times 70 mL), 1.2 M HCl (2 \times 70 mL), H_2O (70 mL), 0.5 M NaHCO_3 (2 \times 70 mL), and H_2O (70 mL). After drying over NaSO_4 , the solvent was removed under reduced pressure, giving white solid 11-bromoundecanoic peroxide as crude, which was used in the next step without delay. The crude product (3.51 g, 12.5 mmol), coenzyme Q_0 (1.31 g, 7.19 mmol), and acetic acid (60 mL) was synthesized by stirring for 20 h at 100 °C²² (see Scheme 5). After cooling to room temperature, the reaction mixture was diluted with diethyl ether (300 mL), washed with H_2O (3 \times 200 mL), 1 M HCl (3 \times 250 mL), 0.5 M NaHCO_3 (3 \times 250 mL), and H_2O (3 \times 200 mL), and dried over NaSO_4 . Removal of the solvent under reduced pressure obtained a reddish solid. The residue was purified by silica gel column chromatography to afford **9** as a red oil (1.07g, 37%). $^1\text{H NMR}$ (500 MHz, CDCl_3 , 298 K): 4.00 (s, 6H, 2 \times $-\text{OCH}_3$), 3.43 (t, 2H, $-\text{CH}_2\text{Br}$), 2.45 (t, 2H, Ar- CH_2-), 2.05 (s, 3H, $-\text{CH}_3$), 1.87 (s, 2H, $-\text{CH}_2-\text{CH}_2\text{Br}$), 1.25–1.47 (m, 14H, $-(\text{CH}_2)_7-$) ppm; MS (EI): calculated 400.2/402.2; found 400.12/402.12.

Acknowledgements

We are grateful for help from Drs. Jia Li and Jing-Ya Li of the Chinese National Center for Drug Screening, Shanghai Institute of Materia Medica, Shanghai Institutes for Biological Sciences, Chinese Academy of Sciences. This research was supported by the Ministry of Health (2009ZX 10004-301), the open research fund from Key Lab of Analytical Chemistry for Life Science of Nanjing University, the Major Research plan of the Natural Science Foundation of China (Grant No. 91027035) and the Fundamental Research Funds for the Central Universities (Grant No. WK1013002). Y.T.L. is supported by The Program for Professor of Special Appointment (Eastern Scholar) at Shanghai Institutions of Higher Learning.

Supplementary data

These data include electrochemical reduction mechanism of ubiquinone; cytotoxicity of **UQAs** toward normal cell; NMR and

Mass spectra of **UQAs** described in this article. Supplementary data related to this article are available free of charge through Internet. Supplementary data related to this article can be found online at doi:10.1016/j.tet.2011.06.026.

References and notes

1. Olgun, A.; Akman, S.; Tezcan, S.; Kutluay, T. *Med. Hypotheses* **2003**, *60*, 325.
2. Jeya, M.; Moon, H. J.; Lee, J. L.; Kim, I. W.; Lee, J. K. *Appl. Microbiol. Biotechnol.* **2010**, *85*, 1653.
3. Lass, A.; Agarwal, S.; Sohal, R. S. *J. Biol. Chem.* **1997**, *272*, 19199.
4. Matthews, R. T.; Yang, L.; Browne, S.; Baik, M.; Beal, M. F. *Proc. Natl. Acad. Sci. U.S.A.* **1998**, *95*, 8892.
5. Do, T. Q.; Schultz, J. R.; Clarke, C. F. *Proc. Natl. Acad. Sci. U.S.A.* **1996**, *93*, 7534.
6. Nonella, M. J. *Phys. Chem. B* **1998**, *102*, 4217.
7. Paddock, M. L.; Feher, G.; Okamura, M. Y. *Proc. Natl. Acad. Sci. U.S.A.* **2000**, *97*, 1548.
8. Turunen, M.; Olsson, J.; Dallner, G. *Biochim. Biophys. Acta* **2004**, *1660*, 171.
9. Costentin, C. *Chem. Rev.* **2008**, *108*, 2145.
10. Quan, M.; Sanchez, D.; Wasylkiw, M. F.; Smith, D. K. *J. Am. Chem. Soc.* **2007**, *129*, 12847.
11. Wang, X. W.; Ma, W.; Ying, Y. L.; Liang, J.; Long, Y.-T. *Chem.—Asian J.* **2011**, *4*, 949.
12. Yu, C. A.; Gu, L. Q.; Lin, Y. Z.; Yu, L. *Biochemistry* **1985**, *24*, 3897.
13. Hayashi, T.; Asai, T.; Hokazono, H.; Ogoshi, H. *J. Am. Chem. Soc.* **1993**, *115*, 12210.
14. Li, W. W.; Hellwig, P.; Ritter, M.; Haehnel, W. *Chem.—Eur. J.* **2006**, *12*, 7236.
15. Smith, R. A. J.; Kelso, G. F.; James, A. M.; Murphy, M. P. *Methods Enzymol.* **2004**, *382*, 45.
16. Roura-Pérez, G.; Quiroz, B.; Aguilar-Martínez, M.; Frontana, C.; Solano, A.; González, I.; Bautista-Martínez, J. A.; Jiménez-Barbero, J.; Cuevas, G. *J. Org. Chem.* **2007**, *72*, 1883.
17. Madej, M. G.; Nasiri, H. R.; Hilgendorff, N. S.; Schwalbe, H.; Unden, G.; Lancaster, C. R. D. *Biochemistry* **2006**, *45*, 15049.
18. Schlosser, M.; Schaub, B. *Chimia* **1982**, *36*, 396.
19. Jung, Y. S.; Joe, B. Y.; Cho, S. J.; Konishi, Y. *Bioorg. Med. Chem. Lett.* **2005**, *15*, 1125.
20. Williams, D. B. G.; Shaw, M. L. *Tetrahedron* **2007**, *63*, 1624.
21. Kikumasa, S.; Seiichi, I.; Ryohei, Y. *J. Org. Chem.* **1972**, *37*, 1889.
22. Kelso, G. F.; Porteous, C. M.; Coulteri, C. V.; Hughes, G.; Porteous, W. K.; Ledgerwood, E. C.; Smith, R. A. J.; Murphy, M. P. *J. Biol. Chem.* **2001**, *276*, 4588.
23. Gupta, N.; Linschitz, H. *J. Am. Chem. Soc.* **1997**, *119*, 6384.
24. Lehmann, M. W.; Evans, D. H. *J. Electroanal. Chem.* **2001**, *500*, 12.
25. Bard, A. J.; Faulkner, L. R. In *Electrochemical Methods: Fundamentals and Applications*; WILEY & Sons: New York, NY, 2001; Vol. 2, p 111.
26. Sumner, J. J.; Creager, S. E. *J. Am. Chem. Soc.* **2000**, *122*, 11914.
27. Bauscher, M.; Mantele, W. *J. Phys. Chem.* **1992**, *96*, 11101.
28. Manda, S.; Nakanishi, I.; Ohkubo, K.; Yakumaru, H.; Matsumoto, K.; Ozawa, T.; Ikota, N.; Fukuzumi, S.; Anzai, K. *Org. Biomol. Chem.* **2007**, *5*, 3951.
29. Gilroy, J. B.; McKinnon, S. D. J.; Koivisto, B. D.; Hicks, R. G. *Org. Lett.* **2007**, *9*, 4837.
30. Morrison, L. E.; Schelhom, J. E.; Cotton, T. M.; Bering, C. L.; Loach, P. A. In *Function of Quinones in Energy Conserving Systems*; Trumpower, B. L., Ed.; Academic: New York, NY, 1982; p 60.
31. Guo, Q.; Corbett, J. T.; Yue, G.; Fann, Y. C.; Qian, S. Y.; Tomer, K. B.; Mason, R. P. *J. Biol. Chem.* **2002**, *277*, 6104.
32. Kim, C.; Kim, N.; Joo, H.; Youm, J. B.; Park, W. S.; Cuong, D. V.; Park, Y. S.; Kim, E.; Min, C. K.; Han, J. *J. Cardiovasc. Pharmacol.* **2005**, *46*, 200.
33. Flueraru, M.; So, R.; Willmore, W. G.; Poulter, M. O.; Durst, T.; Charron, M.; Wright, J. S. *Chem. Res. Toxicol.* **2006**, *19*, 1221.
34. Gutierrez, P. L. *Front. Biosci.* **2000**, *5*, 629.
35. Valderrama, J. A.; Ibacache, J. A.; Arancibia, V.; Rodriguez, J.; Theoduloz, C. *Bioorg. Med. Chem.* **2009**, *17*, 2894.
36. Bair, J. S.; Palchaudhuri, R.; Hergenrother, P. J. *J. Am. Chem. Soc.* **2010**, *132*, 5469.
37. Long, Y. T.; Yu, Z. H.; Chen, H. Y. *Electrochem. Commun.* **1999**, *1*, 194.
38. Cayuela, J.; Manas, A. R. B.; James, A. M.; Smith, R. A. J.; Murphy, M. P. *FEBS Lett.* **2004**, *571*, 9.
39. Carpino, L. A.; Triolo, S. A.; Berglund, R. A. *J. Org. Chem.* **1989**, *54*, 3303.
40. Lipshutz, B. H.; Bülow, G.; Lowe, R. F.; Stevens, K. L. *Tetrahedron* **1996**, *52*, 7265.
41. Ohkawa, S.; Terao, S.; Terashit, Z.; Shibouta, Y.; Nishikawa, K. *J. Med. Chem.* **1991**, *34*, 267.
42. Alison, M. D.; Andrew, D. A. *Org. Biomol. Chem.* **2004**, *2*, 2371.